

Prediction of an $I(J^P) = 0(1^-)$ $\bar{b}b\bar{u}d$ Tetraquark Resonance Close to the B^*B^* Threshold Using Lattice QCD Potentials

Jakob Hoffmann ^{*1} and Marc Wagner ^{†1,2}

¹Institut für Theoretische Physik, Goethe Universität Frankfurt am Main, Max-von-Laue-Straße 1, D-60438 Frankfurt am Main, Germany

²Helmholtz Research Academy Hesse for FAIR, Campus Riedberg, Max-von-Laue-Straße 12, D-60438 Frankfurt am Main, Germany

December 09, 2024

Abstract

We use antistatic-antistatic potentials computed with lattice QCD and a coupled-channel Born-Oppenheimer approach to explore the existence of a $\bar{b}b\bar{u}d$ tetraquark resonance with quantum numbers $I(J^P) = 0(1^-)$. A pole in the T matrix signals a resonance with mass $m = 2m_B + 94.0_{-5.4}^{+1.3}$ MeV and decay width $\Gamma = 140_{-66}^{+86}$ MeV, i.e. very close to the B^*B^* threshold. We also compute branching ratios, which clearly indicate that this resonance is mainly composed of a B^*B^* meson pair with a significantly smaller BB contribution. By varying the potential matrix responsible for the coupling of the BB and the B^*B^* channel as well as the b quark mass, we provide additional insights and understanding concerning the formation and existence of the resonance. We also comment on the importance of our findings and the main takeaways for a possible future full lattice QCD investigation of this $I(J^P) = 0(1^-)$ $\bar{b}b\bar{u}d$ tetraquark resonance.

I Introduction

There has been a long standing effort to experimentally find and theoretically predict exotic mesons, i.e. mesons with a more complicated structure than just a quark-antiquark pair. Tetraquarks, a specific class of exotic mesons, are color neutral states of two quarks and two antiquarks. They were first proposed almost 50 years ago in Ref. [1]. A very clear experimental verification of the existence of tetraquarks was the detection of the electrically charged Z_b and Z_c states around 10 years ago (see Refs. [2–7]). Their masses and decay channels strongly suggest a heavy $\bar{b}b$ or $\bar{c}c$ pair, while their non-vanishing electrical charge implies the presence of an additional light quark-antiquark pair. Recently, another very interesting and clear tetraquark system was found at LHCb, the $T_{cc}(3875)^+$ [8]. This state is composed of two heavy c quarks and two light antiquarks and has quantum numbers $I(J^P) = 0(1^+)$. Its mass is located slightly below the lightest meson-meson threshold and it is, thus, almost QCD-stable.

From the theoretical perspective antiheavy-antiheavy-light-light ($\bar{Q}\bar{Q}qq$) systems (or equivalently heavy-heavy-antilight-antilight states) are particularly interesting, since they are somewhat simpler to study than some of the more common $\bar{Q}Q\bar{q}q$ systems, mainly because of two reasons: (1) quark-antiquark annihilation is not possible; (2) they can only decay into two heavy-light mesons, but not into quarkonium and a light meson. There are quite a number of papers studying such $\bar{Q}\bar{Q}qq$ tetraquarks based on a variety of phenomenological or QCD-based approaches including quark models [9–30], sum rules [31–38], effective field theories [39–45] and functional methods [46–48].

The first lattice QCD studies of $\bar{Q}\bar{Q}qq$ tetraquarks, mostly of the $\bar{b}b\bar{u}d$ tetraquark with quantum numbers $I(J^P) = 0(1^+)$, which is the bottom counterpart of the experimentally found $T_{cc}(3875)^+$, were based on antistatic-antistatic potentials [49–53]. For heavy quark masses significantly larger than the typical QCD scale relevant for the dynamics of the light quarks, a $\bar{Q}\bar{Q}qq$ tetraquark system can be described by a non-relativistic Hamiltonian in the so-called Born-Oppenheimer approximation (see e.g. Ref. [40]). The first crude predictions of that type just used a single $\bar{Q}\bar{Q}$ potential from lattice QCD and a simple single-channel Schrödinger equation and, thus, did not distinguish between B and B^* mesons [52–54]. For example, Ref. [53] found a binding energy of 90_{-43}^{+36} MeV for the $I(J^P) = 0(1^+)$ $\bar{b}b\bar{u}d$ tetraquark at physically light u and d quark masses. Later this approach was refined, by deriving a coupled-channel Schrödinger equation taking into account both an attractive and a repulsive $\bar{Q}\bar{Q}$

*jhoffmann@itp.uni-frankfurt.de

†mwagner@itp.uni-frankfurt.de

potential and the mass difference of B and B^* . This inclusion of heavy spin effects resulted in a significantly reduced binding energy 59^{+30}_{-38} MeV [55], indicating the importance of proper multi-channel equations in the Born-Oppenheimer approach. For a recent and very comprehensive discussion and application of Born-Oppenheimer effective field theory to arbitrary XYZ exotic states we refer to Ref. [45].

$\bar{b}b\bar{u}d$ tetraquarks with quantum numbers $I(J^P) = 0(1^+)$, as well as related systems with flavor content $\bar{b}\bar{b}us$, $\bar{b}\bar{c}ud$ and $\bar{c}\bar{c}ud$, have meanwhile also been investigated rigorously within full lattice QCD by several independent groups (see Refs. [56–70]). These computations point towards a binding energy of around 100 MeV for the $I(J^P) = 0(1^+)$ $\bar{b}b\bar{u}d$ tetraquark, which is in fair agreement with the previously mentioned result 59^{+30}_{-38} MeV from the refined Born-Oppenheimer approach [55].

Full lattice QCD computations with either $\bar{Q}\bar{Q} = \bar{b}\bar{b}$ or $\bar{Q}\bar{Q} = \bar{b}\bar{c}$ focus mainly on QCD-stable $\bar{Q}\bar{Q}qq$ tetraquarks¹. However, in addition to these stable states there might also exist short-lived tetraquark resonances. For example in Ref. [71] a $\bar{b}b\bar{u}d$ tetraquark resonance with quantum numbers $I(J^P) = 0(1^-)$ was predicted using lattice QCD potentials and the Born-Oppenheimer approach. There, a simple single-channel scattering problem was solved and a resonance was found 17^{+4}_{-4} MeV above the lightest meson-meson threshold. Since in that work the B and the B^* mesons were treated as degenerate in mass, it could only be speculated, whether the predicted resonance should be expected near the BB or the B^*B^* threshold or somewhere in-between. In the present work we combine the refined coupled-channel Born-Oppenheimer approach from Ref. [55] with scattering theory and thoroughly search for the $I(J^P) = 0(1^-)$ $\bar{b}b\bar{u}d$ tetraquark resonance in the energy region between the BB threshold and slightly above the B^*B^* threshold. Preliminary results obtained at an early stage of this project indicated that there is no resonance close to the BB threshold [72]. In the following sections we give theoretical arguments, why the resonance crudely predicted in Ref. [71] should be expected near the B^*B^* threshold, and present numerical results on the resonance mass confirming this expectation. Moreover, we compute branching ratios indicating that this resonance is mainly a B^*B^* system with a significantly smaller BB component.

This paper is structured as follows. In Section II we review the computation of antistatic-antistatic potentials with lattice QCD. In Section III we derive a 16×16 coupled-channel Schrödinger equation for these potentials. We also decompose this equation into smaller independent blocks corresponding to definite spin quantum numbers. In Section IV we use standard techniques from non-relativistic scattering theory to relate the relevant coupled-channel Schrödinger equation to the elements of the T matrix. In Section V we solve the Schrödinger equation numerically and search for poles of the T matrix in the complex energy plane. This provides the mass, the decay width and the BB and B^*B^* branching ratios of the $I(J^P) = 0(1^-)$ $\bar{b}b\bar{u}d$ tetraquark resonance. We also explore the dependence of our results on the potential matrix responsible for the coupling of the BB and the B^*B^* channel as well as on the heavy quark mass, to provide additional insights and understanding concerning the formation and existence of a resonance of that type. We conclude in Section VI.

II $\bar{Q}\bar{Q}qq$ Static Potentials from Lattice QCD

The Born-Oppenheimer approach for antiheavy-antiheavy-light-light tetraquarks consists of two independent steps. In the first step one uses the static-quark approximation for the heavy antiquarks $\bar{Q}\bar{Q}$ and computes the corresponding antistatic-antistatic potentials in the presence of two light quarks qq with lattice QCD. In this section we briefly review this first step to keep the paper self-contained (see Ref. [53] for more details) and introduce the relevant notation. In the second step of the Born-Oppenheimer approach, one inserts the static potentials obtained in step 1 into coupled-channel Schrödinger equations to predict masses and properties of QCD-stable bound states or resonances. At this stage we also include the spin of the heavy \bar{b} quarks. The main focus of this work is on step 2, for which we extend methods developed in Ref. [55] for the QCD-stable $\bar{b}b\bar{u}d$ tetraquark with quantum numbers $I(J^P) = 0(1^+)$ to a $\bar{b}b\bar{u}d$ tetraquark resonance with quantum numbers $I(J^P) = 0(1^-)$.

In Refs. [50, 53] antistatic-antistatic potentials were computed for isospin $I = 0, 1$. These potentials were extracted from the asymptotic t behavior of Euclidean two-point correlation functions

$$C(t) = \langle \Omega | \mathcal{O}^\dagger(\vec{r}_1, \vec{r}_2, t) \mathcal{O}(\vec{r}_1, \vec{r}_2, 0) | \Omega \rangle. \quad (1)$$

In this work we are exclusively interested in $I = 0$, for which the relevant operators are

$$\mathcal{O}(\vec{r}_1, \vec{r}_2) = (\mathbf{C}\mathbb{L})_{AB} (\mathbf{C}\mathbb{S})_{CD} \left(\bar{Q}_C^a(\vec{r}_1) u_A^a(\vec{r}_1) \right) \left(\bar{Q}_D^b(\vec{r}_2) d_B^b(\vec{r}_2) \right) - (u \leftrightarrow d), \quad (2)$$

¹An exception is Ref. [66], where indications for the existence of $\bar{b}\bar{c}ud$ tetraquark resonances were found.

where \vec{r}_1 and \vec{r}_2 denote the positions of the static antiquarks \bar{Q} , $\mathbf{C} = \gamma_0\gamma_2$ is the charge conjugation matrix, $a, b = 1, 2, 3$ are color indices, $A, B, C, D = 1, 2, 3, 4$ are spin indices, \mathbb{L} is the light quark spin matrix and \mathbb{S} is the heavy quark spin matrix.

There are just 4 linearly independent possibilities for the heavy quark spin matrix,

$$\mathbb{S} \in \{(\mathbb{1} + \gamma_0)\gamma_5, (\mathbb{1} + \gamma_0)\gamma_j\} \quad (3)$$

with $j = 1, 2, 3$, because static quark spinors have only two components. Since static potentials are degenerate with respect to the heavy quark spins, the concrete choice of \mathbb{S} is irrelevant in this section. It will, however, become important in Section III, when we set up coupled-channel Schrödinger equations and distinguish B and B^* mesons.

For the light quark spin matrix there are 16 linearly independent possibilities, $\mathbb{L} \in \{(\mathbb{1} \pm \gamma_0)\gamma_5, (\mathbb{1} \pm \gamma_0)\gamma_j, (\mathbb{1} \pm \gamma_0)\mathbb{1}, (\mathbb{1} \pm \gamma_0)\gamma_5\gamma_j\}$, chosen such that the corresponding trial states $\mathcal{O}^\dagger(\vec{r}_1, \vec{r}_2)|\Omega\rangle$ have definite quantum numbers $|j_z|$, \mathcal{P} and \mathcal{P}_x . $|j_z|$ is the total angular momentum of the light quarks and gluons in the direction of the $\bar{Q}\bar{Q}$ separation axis (for simplicity one can choose the z axis), \mathcal{P} denotes parity and \mathcal{P}_x the behavior under reflection along an axis perpendicular to the separation axis (e.g. the x axis). At large $\bar{Q}\bar{Q}$ separations the $\bar{Q}\bar{Q}qq$ system will consist of two heavy light mesons, either B , B^* , B_0^* and/or B_1^* . In this work we are only interested in the negative parity mesons B and B^* , but not their positive parity partners B_0^* and/or B_1^* , which are around 500 MeV heavier. Thus, we just need to consider potentials with asymptotic values of two times the B and/or B^* meson mass ($m_B = m_{B^*}$ for static heavy quarks), but not with higher asymptotic values corresponding to a negative and a positive parity meson or two positive parity mesons. One can show that the relevant choices for the light quark spin matrix are then limited to

$$\mathbb{L} \in \{(\mathbb{1} + \gamma_0)\gamma_5, (\mathbb{1} + \gamma_0)\gamma_j\} \quad (4)$$

(see Ref. [53] for details), which lead to two different potentials. $\mathbb{L} = (\mathbb{1} + \gamma_0)\gamma_5$ corresponds to a strongly attractive potential, denoted as $V_5(r)$, whereas $\mathbb{L} = (\mathbb{1} + \gamma_0)\gamma_j$ corresponds to a significantly weaker repulsive potential, denoted as $V_j(r)$ ($r = |\vec{r}_2 - \vec{r}_1|$ is the $\bar{Q}\bar{Q}$ separation).

The lattice QCD results for $V_5(r)$ and $V_j(r)$ from Ref. [53] (with two times the lightest static-light meson mass subtracted), extrapolated to the physical pion mass $m_\pi \approx 140$ MeV, can be consistently parameterized by

$$V_X(r) = -\frac{\alpha_X}{r} e^{-(r/d_X)^2} \quad , \quad X = 5, j \quad (5)$$

with parameters $\alpha_5 = 0.34 \pm 0.03$, $d_5 = 0.45_{-0.10}^{+0.12}$ fm, $\alpha_j = -0.10 \pm 0.07$ and $d_j = (0.28 \pm 0.017)$ fm determined by χ^2 -minimizing fits in Refs. [53, 55]. These potential parameterizations are shown in Figure 1. For small $\bar{Q}\bar{Q}$ separations the potentials are dominated by 1-gluon exchange between the static quarks and, thus, are proportional to $1/r$. For large separations, the potentials are exponentially screened and represent rather weak residual meson-meson interactions.

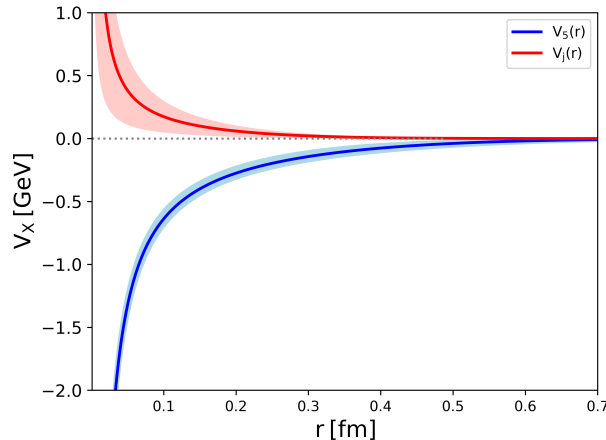


Figure 1: Potential parameterizations V_5 and V_j of lattice QCD results from Ref. [53] as functions of the $\bar{Q}\bar{Q}$ separation r .

III Coupled-Channel Schrödinger Equation for $I(J^P) = 0(1^-)$

III.I 16×16 Coupled-Channel Schrödinger Equation

The potentials $V_5(r)$ and $V_j(r)$ discussed in Section II are independent of the static quark spins. Now we include heavy quark spin effects in our approach by setting the asymptotic potential values to the corresponding two meson thresholds, $2m_B$, $m_B + m_{B^*}$ and $2m_{B^*}$, respectively. We take the meson masses m_B and m_{B^*} from experiments [73], most importantly the mass difference $m_{B^*} - m_B = 45 \text{ MeV}$.

Following Ref. [55] a 16×16 Hamiltonian can be defined as

$$H = H_0 + H_{\text{int}} \quad (6)$$

with a free part

$$H_0 = M \otimes \mathbb{1}_{4 \times 4} + \mathbb{1}_{4 \times 4} \otimes M + \frac{\vec{p}_1^2 + \vec{p}_2^2}{2m_b} \quad (7)$$

essentially describing non-interacting B and B^* mesons. \vec{p}_1 and \vec{p}_2 are the momenta of the heavy \bar{b} quarks, m_b denotes the b quark mass and $M = \text{diag}(m_B, m_{B^*}, m_{B^*}, m_{B^*})$ is a 4×4 diagonal matrix containing the masses of B and B^* mesons. The corresponding free Schrödinger equation in the center of mass frame is a partial differential equation for the relative coordinate of the \bar{b} quarks $\vec{r} = \vec{r}_2 - \vec{r}_1$,

$$H_0 \vec{\Psi}(\vec{r}) = E \vec{\Psi}(\vec{r}) \quad , \quad H_0 = M \otimes \mathbb{1}_{4 \times 4} + \mathbb{1}_{4 \times 4} \otimes M + \frac{\vec{p}^2}{2\mu} \quad (8)$$

with the reduced mass $\mu = m_b/2$. The wave function $\vec{\Psi}(\vec{r})$ has 16 components, where each component is associated with a specific meson-meson pair,

$$\vec{\Psi} \equiv (BB, BB_x^*, BB_y^*, BB_z^* \quad , \quad B_x^*B, B_x^*B_x^*, B_x^*B_y^*, B_x^*B_z^* \quad , \quad B_y^*B, B_y^*B_x^*, B_y^*B_y^*, B_y^*B_z^* \quad , \quad B_z^*B, B_z^*B_x^*, B_z^*B_y^*, B_z^*B_z^*)^T \quad (9)$$

with the indices x, y, z denoting the three possible spin orientations of a B^* meson.

The interacting part H_{int} contains the potentials $V_5(r)$ and $V_j(r)$. It is a 16×16 non-diagonal matrix, which couples the 16 independent partial differential equations from Eq. (8). This is so, because the potentials $V_5(r)$ and $V_j(r)$ do not correspond to simple combinations of two specific mesons, but rather to linear combinations of several B and/or B^* meson pairs as we work out in detail in the following. To derive the mathematical structure of H_{int} , we use

$$H_{\text{int}} = T^{-1} V_{\text{diag}}(r) T \quad , \quad V_{\text{diag}} = \text{diag}(\underbrace{V_5(r), \dots, V_5(r)}_{4 \times}, \underbrace{V_j(r), \dots, V_j(r)}_{12 \times}) \quad (10)$$

as a starting point. T is a 16×16 transformation matrix, whose entries are determined by rewriting the interpolating operators defined in equation (2) in terms of combinations of heavy-light mesons. In other words, T transforms the 16 operators (2) with \mathbb{S} and \mathbb{L} chosen according to Eqs. (3) and (4) to the 16 meson-meson combinations defined in Eqs. (8) and (9) via the Schrödinger equation and the corresponding 16-component wave function. The entries of T can be obtained by expressing the operators (2) in terms of quark-antiquark combinations, not only in color space, but also in spin space, using Fierz identities,

$$\mathcal{O}(\vec{r}_1, \vec{r}_2) = \mathbb{G}(\mathbb{S}, \mathbb{L})_{AB} \left(\bar{Q}(\vec{r}_1) \Gamma_A u(\vec{r}_1) \right) \left(\bar{Q}(\vec{r}_2) \Gamma_B d(\vec{r}_2) \right) - (u \leftrightarrow d) \quad (11)$$

with coefficients

$$\mathbb{G}(\mathbb{S}, \mathbb{L})_{AB} = \frac{1}{16} \text{Tr} \left((\mathbb{C}\mathbb{S})^T \Gamma_A^T (\mathbb{C}\mathbb{L}) \Gamma_B \right). \quad (12)$$

The implicit sums over A and B in Eq. (11) are over four matrices each, i.e. $\Gamma_A, \Gamma_B \in \{(\mathbb{1} + \gamma_0)\gamma_5, (\mathbb{1} + \gamma_0)\gamma_j\}$, where $\bar{Q}\Gamma_A q$ with $\Gamma_A = (\mathbb{1} + \gamma_0)\gamma_5$ represents a B meson (quantum numbers $J^P = 0^-$) and $\bar{Q}\Gamma_A q$ with $\Gamma_A = (\mathbb{1} + \gamma_0)\gamma_j$ represents one of the three possible spin orientations of a B^* meson (quantum numbers $J^P = 1^-$). The entries of the matrix T are given by the coefficients $\mathbb{G}(\mathbb{S}, \mathbb{L})_{AB}$:

- The row of T is given by the choice of \mathbb{S} and \mathbb{L} and a mapping consistent with the right equation in (10). This requires that rows 1 to 4 correspond to $\mathbb{L} = (\mathbb{1} + \gamma_0)\gamma_5$ and rows 5 to 16 to $\mathbb{L} = (\mathbb{1} + \gamma_0)\gamma_j$. The mapping with respect to \mathbb{S} is not unique. For example, one can define that rows 1, 5, 9, 13 correspond to $\mathbb{S} = (\mathbb{1} + \gamma_0)\gamma_5$, rows 2, 6, 10, 14 correspond to $\mathbb{S} = (\mathbb{1} + \gamma_0)\gamma_1$, etc.

- The column of T is given by the indices A and B and the mapping (9).

In total, we now have the Schrödinger equation

$$H\vec{\Psi}(\vec{r}) = (H_0 + H_{\text{int}})\vec{\Psi}(\vec{r}) = E\vec{\Psi}(\vec{r}) \quad (13)$$

with H_0 from Eq. (8) and H_{int} from Eq. (10). This is a coupled-channel partial differential equation in the relative coordinate \vec{r} . The 16 equations are coupled by the non-vanishing off-diagonal elements of H_{int} .

III.II Radial 1×1 and 2×2 Coupled-Channel Schrödinger Equations

Since there is no spin-orbit coupling in our Hamiltonian, the orbital angular momentum operators \vec{L}^2 and L_z commute with H . Thus, L and L_z , representing the relative orbital angular momentum of the two \bar{b} quarks, can be used as quantum numbers. This allows to write the wave function as a product of a radial wave function and a spherical harmonic function, $\vec{\Psi}(\vec{r}) = \vec{\varphi}_L(r)Y_{L,L_z}(\theta, \phi)$, and to simplify the Schrödinger Equation (13) to a radial Schrödinger Equation, i.e. an ordinary differential equation in the $\bar{b}\bar{b}$ separation $r = |\vec{r}|$.

We denote the spin of both, the light and the heavy quarks, represented by the 16 components of the wave function as specified in Eq. (9), by \vec{S} . One can show that \vec{S}^2 and S_z commute with H , \vec{L}^2 and L_z . Thus, in addition to L and L_z one can also use S and S_z as quantum numbers. As a consequence, one can decouple the 16×16 radial Schrödinger equation into smaller blocks labeled by S and S_z . Standard spin coupling of four spin 1/2 particles is given by $\mathbf{2} \otimes \mathbf{2} \otimes \mathbf{2} \otimes \mathbf{2} = \mathbf{2} \oplus \mathbf{9} \oplus \mathbf{5}$, where $\mathbf{2}$ on the right hand side denotes a 2×2 block with $S = 0$, $\mathbf{9}$ denotes 3 degenerate 3×3 blocks with $S = 1$ and $\mathbf{5}$ denotes 5 degenerate 1×1 blocks with $S = 2$. The decoupling was already worked out in Ref. [55]. In the following we just summarize the resulting equations.

Radial Schrödinger Equation for $S = 0$

For $S = 0$ there is a single 2×2 equation,

$$\left(\begin{pmatrix} 2m_B & 0 \\ 0 & 2m_{B^*} \end{pmatrix} - \frac{\nabla^2}{2\mu} + H_{\text{int},S=0} \right) \vec{\varphi}_{L,S=0}(r) = E\vec{\varphi}_{L,S=0}(r) \quad (14)$$

with

$$\nabla^2 = \frac{d^2}{dr^2} + \frac{2}{r} \frac{d}{dr} - \frac{L(L+1)}{r^2} \quad (15)$$

and

$$H_{\text{int},S=0} = \frac{1}{4} \begin{pmatrix} V_5(r) + 3V_j(r) & \sqrt{3}(V_5(r) - V_j(r)) \\ \sqrt{3}(V_5(r) - V_j(r)) & 3V_5(r) + V_j(r) \end{pmatrix}. \quad (16)$$

The 2 components of the wave function represent the following meson-meson combinations:

$$\vec{\varphi}_{L,S=0} \equiv \left(BB, \frac{1}{\sqrt{3}}\vec{B}^*\vec{B}^* \right)^T = \left(BB, \frac{1}{\sqrt{3}}(B_x^*B_x^* + B_y^*B_y^* + B_z^*B_z^*) \right)^T. \quad (17)$$

Radial Schrödinger Equations for $S = 1$

There are 3 identical 3×3 equations for $S = 1$ corresponding to $S_z = -1, 0, +1$. Each of these 3×3 equations can be decoupled further, into a 1×1 equation (i.e. a single equation), which is symmetric under meson exchange, and a 2×2 equation, which is antisymmetric under B/B^* meson exchange.

The 1×1 equation is

$$\left(m_B + m_B^* - \frac{\nabla^2}{2\mu} + H_{\text{int},S=1}^{(1 \times 1)} \right) \varphi_{L,S=1,S_z}^{(1 \times 1)}(r) = E\varphi_{L,S=1,S_z}^{(1 \times 1)}(r) \quad (18)$$

with

$$H_{\text{int},S=1}^{(1\times 1)} = V_j(r) \quad , \quad \varphi_{L,S=1,S_z}^{(1\times 1)}(r) \equiv \frac{1}{\sqrt{2}} \left(B_{S_z}^* B + B B_{S_z}^* \right). \quad (19)$$

The 2×2 equation is

$$\left(\begin{pmatrix} m_B + m_{B^*} & 0 \\ 0 & 2m_{B^*} \end{pmatrix} - \frac{\nabla^2}{2\mu} + H_{\text{int},S=1}^{(2\times 2)} \right) \bar{\varphi}_{L,S=1,S_z}^{(2\times 2)}(r) = E \bar{\varphi}_{L,S=1,S_z}^{(2\times 2)}(r) \quad (20)$$

with

$$H_{\text{int},S=1}^{(2\times 2)} = \frac{1}{2} \begin{pmatrix} V_5(r) + V_j(r) & V_5(r) - V_j(r) \\ V_5(r) - V_j(r) & V_5(r) + V_j(r) \end{pmatrix} \quad , \quad \bar{\varphi}_{L,S=1,S_z}^{(2\times 2)}(r) \equiv \left(\frac{1}{\sqrt{2}} \left(B_{S_z}^* B - B B_{S_z}^* \right) \quad , \quad T_{1,S_z}(\vec{B}^*, \vec{B}^*) \right)^T, \quad (21)$$

where T_{1,S_z} is a spherical tensor representing the coupling of two B^* mesons to $S = 1$ with z component S_z .

Radial Schrödinger Equations for $S = 2$

There are 5 identical 1×1 equations for $S = 2$ corresponding to $S_z = -2, -1, 0, +1, +2$,

$$\left(2m_{B^*} - \frac{\nabla^2}{2\mu} + H_{\text{int},S=2} \right) \varphi_{L,S=2,S_z}(r) = E \varphi_{L,S=2,S_z}(r) \quad (22)$$

with

$$H_{\text{int},S=2} = V_j(r) \quad , \quad \varphi_{L,S=2,S_z}(r) \equiv T_{2,S_z}(\vec{B}^*, \vec{B}^*), \quad (23)$$

where T_{2,S_z} is a spherical tensor representing the coupling of two B^* mesons to $S = 2$ with z component S_z .

III.III Selecting the Coupled-Channel Schrödinger Equation for $I(J^P) = 0(1^-)$

The formalism we developed so far in this section and the resulting coupled-channel Schrödinger equations (14), (18), (20) and (22) are applicable to $\bar{b}b u d$ systems with arbitrary quantum numbers I and L . Since our goal in this work is a refined study of the $I(J^P) = 0(1^-)$ tetraquark resonance predicted in Ref. [55], which has orbital angular momentum 1, we fix $L = 1$, in particular in Eq. (15), for the remainder of this work.

In the following we discuss, which of the four equations (14), (18), (20) and (22) has to be selected to study the $I(J^P) = 0(1^-)$ tetraquark resonance from Ref. [55] in a refined way with effects due to the heavy quark spins and the corresponding B and B^* mass splitting included. We start by collecting all combinations of isospin I , light quark spin S_q , light color, heavy color, orbital angular momentum of the heavy quarks $L = 1$, heavy quark spin S_Q , total spin S (with $\vec{S} = \vec{S}_q + \vec{S}_Q$) and total angular momentum J (with $\vec{J} = \vec{L} + \vec{S}$) allowed by the Pauli principle and by color confinement of QCD (see Table 1). There are two possibilities for isospin, $I = 0, 1$, as well as for light quark spin, $S_q = 0, 1$ (column 1 and 2). Moreover, we fix $L = 1$ (column 5), as already stated. The remaining entries in that table are consequences of the Pauli principle and of color confinement as discussed in the following items.

- color (qq):
Since the light quarks are fermions, they must form an antisymmetric combination. Thus, symmetry or antisymmetry with respect to I and to S_q fix the light color to either an antisymmetric $\bar{3}$ or a symmetric 6. For example, an antisymmetric $I = 0$ and an antisymmetric $S_q = 0$ imply an antisymmetric light color $\bar{3}$ (first line in Table 1).
- color ($\bar{b}\bar{b}$):
Color confinement requires a color singlet for the four quarks. Thus, if color (qq) is $\bar{3}$, color ($\bar{b}\bar{b}$) must be 3. If color (qq) is 6, color ($\bar{b}\bar{b}$) must be $\bar{6}$.
- S_Q :
Since the \bar{b} quarks are fermions, they must form an antisymmetric combination. Thus, symmetry or antisymmetry with respect to color ($\bar{b}\bar{b}$) and to $L = 1$ fix S_Q . For example, an antisymmetric color ($\bar{b}\bar{b}$) = 3 and an antisymmetric $L = 1$ imply an antisymmetric heavy quark spin $S_Q = 0$ (first line in Table 1).

- S :
 S is the usual coupling of S_q and S_Q with no further restrictions. The values of S allow to assign the radial Schrödinger equations (14), (18), (20) and (22) to the four lines of Table 1 (last column “equations”). Since $S = 1$ appears only once for $I = 0$, but twice for $I = 1$, it is clear that the 1×1 equation (18) corresponds to $I = 0, S = 1$ and the 2×2 equation (20) to $I = 1, S = 1$. For the 2×2 equations we also note, whether a line in Table 1 corresponds to the attractive potential $V_5(r)$ or the repulsive potential $V_j(r)$. This is directly related to color ($\bar{b}b$) and 1-gluon exchange dominating at small separations, where $\bar{3}$ corresponds to an attractive potential and 6 to a repulsive potential (see e.g. Ref. [53] for a detailed discussion).
- J^P :
 J is the usual coupling of L and S with no further restrictions. Parity $P = -$ in all cases, because both the heavy quarks and the light quarks are in negative parity combinations (see Eqs. (3) and (4)) and orbital angular momentum $L = 1$ also contributes a factor of -1 to P .

light quarks qq			heavy quarks $\bar{b}\bar{b}$			tetraquark $\bar{b}bqq$		equations
I	S_q	color (qq)	color ($\bar{b}\bar{b}$)	L	S_Q	S	J^P	
$0(A)$	$0(A)$	$\bar{3}(A)$	$3(A)$	$1(A)$	$0(A)$	0	1^-	$V_5(r)$ in Eq. (14)
	$1(S)$	$6(S)$	$\bar{6}(S)$		$1(S)$	$0, 1, 2$	$0^-, 1^-, 2^-, 3^-$	$V_j(r)$ in Eq. (14) Eq. (18) Eq. (22)
$1(S)$	$0(A)$	$6(S)$	$\bar{6}(S)$		$1(S)$	1	$0^-, 1^-, 2^-$	$V_j(r)$ in Eq. (20)
	$1(S)$	$\bar{3}(A)$	$3(A)$		$0(A)$	1	$0^-, 1^-, 2^-$	$V_5(r)$ in Eq. (20)

Table 1: Combinations of quantum numbers for $\bar{b}bud$ tetraquark systems with orbital angular momentum $L = 1$ of the two \bar{b} quarks and the corresponding radial Schrödinger equations derived in Section III.II. “(S)” and “(A)” denote symmetric and antisymmetric combinations, respectively.

Now it is almost obvious, which of the radial coupled-channel equations (14), (18), (20) and (22) is appropriate to explore the $I(J^P) = 0(1^-)$ tetraquark resonance predicted in Ref. [55] in a refined way. Since it has $I = 0$, the last two lines of Table 1 can be discarded. Moreover, the equation must contain the attractive potential $V_5(r)$. The only candidate left is the 2×2 equation (14) for $S = 0$. This equation, containing both the attractive $V_5(r)$ and the repulsive $V_j(r)$, is the generalization of the simple 1×1 equation used in Ref. [55], which solely contains $V_5(r)$, and where heavy spin effects were ignored. From now on, we will exclusively focus on Eq. (14).

We close this section by noting that Table 1 is essentially valid for arbitrary odd L . One just has to add $L - 1$ to the entries in column “ L ” and column “ J^P ”. For even L one can follow the same logical steps, which will lead to a somewhat different table already presented and discussed in Ref. [55] (Table I in that reference). Moreover, notice that for $I = 1$ the potentials are different compared to the $I = 0$ case we are focusing on: $V_5(r)$ is repulsive and $V_j(r)$ is attractive, however, significantly less attractive than $V_5(r)$ for $I = 0$, because of the interaction of the two light spins (see Ref. [74]).

IV Scattering Formalism

Now we prepare the coupled-channel Schrödinger equation (14), describing possibly existing $\bar{b}bud$ tetraquark states with $I(J^P) = 0(1^-)$, for numerical scattering analyses, by applying basic techniques from scattering theory. For single-channel equations these techniques are extensively discussed in standard textbooks on quantum mechanics. For a generalization and discussion in the context of coupled-channel equations we refer e.g. to Refs. [75–77].

IV.I Partial Wave Expansion

The radial Schrödinger equation (14) has two coupled-channels, a BB channel and a B^*B^* channel (see Eq. (17)). The corresponding scattering momenta are

$$k_{BB} = \sqrt{2\mu(E - 2m_B)} \quad , \quad k_{B^*B^*} = \sqrt{2\mu(E - 2m_{B^*})}. \quad (24)$$

Both momenta are real for energies $E > 2m_{B^*}$, i.e. above the B^*B^* threshold. For $2m_B < E < 2m_{B^*}$ only the BB channel is open and $k_{B^*B^*}$ is purely imaginary. For $E < 2m_B$, both channels are closed, scattering cannot take place and Eq. (14) describes possibly existing bound states.

These three cases can be treated in the same way, by decomposing the wave function $\vec{\Psi}(\vec{r})$ into incident plane waves and emergent spherical waves and by carrying out a partial wave expansion. For $L = 1$ the radial wave function $\vec{\varphi}_{1,S=0}(r)$ appearing in Eqs. (14) and (17) is then given by

$$\vec{\varphi}_{1,S=0}(r) = \begin{pmatrix} A_{BB}j_1(k_{BB}r) + \chi_{BB}(r)/r \\ A_{B^*B^*}j_1(k_{B^*B^*}r) + \chi_{B^*B^*}(r)/r \end{pmatrix}. \quad (25)$$

A_{BB} and $A_{B^*B^*}$ are the prefactors of the incident BB and B^*B^* waves, respectively. $j_1(k_{BB}r)$ and $j_1(k_{B^*B^*}r)$ denote spherical Bessel functions representing the $L = 1$ contribution to these incident plane waves and $\chi_{BB}(r)/r$ and $\chi_{B^*B^*}(r)/r$ are the radial wave functions of the emergent BB and B^*B^* spherical waves. For large r , where $H_{\text{int},S=0} = 0$, i.e. where the potential matrix (16) vanishes, $\chi_\alpha(r)/r \propto h_1^{(1)}(k_\alpha r)$ with $\alpha = BB, B^*B^*$ and $h_1^{(1)}$ denoting a spherical Hankel function. This allows to define the T matrix (see Eqs. (29) and (30) below).

Inserting the decomposition (25) into Eq. (14) and exploiting that incident plane waves are solutions of the free Schrödinger equation leads to

$$\left(\begin{pmatrix} 2m_B & 0 \\ 0 & 2m_{B^*} \end{pmatrix} - \frac{1}{2\mu} \left(\frac{d^2}{dr^2} - \frac{2}{r^2} \right) + H_{\text{int},S=0} - E \right) \begin{pmatrix} \chi_{BB}(r) \\ \chi_{B^*B^*}(r) \end{pmatrix} = -H_{\text{int},S=0} \begin{pmatrix} A_{BB}rj_1(k_{BB}r) \\ A_{B^*B^*}rj_1(k_{B^*B^*}r) \end{pmatrix}. \quad (26)$$

IV.II Boundary Conditions and Definition of the T Matrix

As usual for radially symmetric problems in 3 dimensional space, the wave functions χ_α close to the origin must be proportional to r^{L+1} , i.e. in our case

$$\chi_\alpha(r) \propto r^2 \quad \text{for } r \rightarrow 0. \quad (27)$$

For large r , where $H_{\text{int},S=0} = 0$, the wave functions χ_α describe exclusively emergent spherical waves and, thus, must be proportional to spherical Hankel functions. This leads to the definition of the 2×2 T matrix,

$$\mathbb{T} = \begin{pmatrix} t_{BB;BB} & t_{BB;B^*B^*} \\ t_{B^*B^*;BB} & t_{B^*B^*;B^*B^*} \end{pmatrix}, \quad (28)$$

where the entries represent scattering amplitudes, which appear in the boundary conditions

$$\chi_\alpha(r) \propto ir t_{BB;\alpha} h_1^{(1)}(k_\alpha r) \quad \text{for } r \rightarrow \infty \text{ and } (A_{BB}, A_{B^*B^*}) = (1, 0) \quad (29)$$

$$\chi_\alpha(r) \propto ir t_{B^*B^*;\alpha} h_1^{(1)}(k_\alpha r) \quad \text{for } r \rightarrow \infty \text{ and } (A_{BB}, A_{B^*B^*}) = (0, 1). \quad (30)$$

Note that Eq. (29) describes a pure BB incident wave, while Eq. (30) describes a pure B^*B^* incident wave. To read off the T matrix entries from Eqs. (29) and (30), one just has to solve Eq. (26) with boundary conditions (27) and (29) for $(A_{BB}, A_{B^*B^*}) = (1, 0)$ as well as with boundary conditions (27) and (30) for $(A_{BB}, A_{B^*B^*}) = (0, 1)$. How this can be done numerically is discussed in Section IV.III.

Poles of the T matrix in the complex energy plane signal either bound states (for $\text{Re}(E_{\text{pole}}) < 2m_B$ and $\text{Im}(E_{\text{pole}}) = 0$) or resonances (for $\text{Re}(E_{\text{pole}}) > 2m_B$ and $\text{Im}(E_{\text{pole}}) < 0$). A pole implies that at least one of the eigenvalues of T diverges or, equivalently, $1/\det(\mathbb{T}) = 0$. We determine the poles of the T matrix in Section V.II by numerically searching for roots of $1/\det(\mathbb{T})$.

IV.III Solving the Coupled-Channel Schrödinger Equation and Computing the T Matrix for Given Energy E

To determine $t_{BB;BB}$ and $t_{BB;B^*B^*}$, the entries in the first row of the T matrix (28) corresponding to an incident BB wave, for given complex energy E , we proceed in the following way:

- (1) We solve the coupled-channel Schrödinger equation (26) for coefficients $(A_{BB}, A_{B^*B^*}) = (1, 0)$ using a standard fourth-order Runge-Kutta method. We start at very small r and use three sets of initial conditions consistent with the boundary conditions (27) to compute three functions:
 - A solution of the inhomogeneous equation (26), denoted as $\vec{\chi}_{\text{inhom}}$, using $\vec{\chi} = (0, 0)^T$ as initial conditions at small r (here and in the following we use the notation $\vec{\chi} = (\chi_{BB}, \chi_{B^*B^*})^T$).
 - Two independent solutions of the homogeneous equation, i.e. Eq. (26) with right hand side replaced by 0, denoted as $\vec{\chi}_{0,a}$ and $\vec{\chi}_{0,b}$, using $\vec{\chi} = (r^2, 0)^T$ and $\vec{\chi} = (0, r^2)^T$ as initial conditions at small r , respectively.

The general numerical solution of the coupled-channel Schrödinger equation (26) for given energy E is then

$$\vec{\chi}_{\text{numerical}}(r) = \vec{\chi}_{\text{inhom}}(r) + a\vec{\chi}_{0,a}(r) + b\vec{\chi}_{0,b}(r) \quad (31)$$

with yet undetermined coefficients a and b .

- (2) In a second step we determine a and b according to the boundary conditions at $r \rightarrow \infty$, Eq. (29), i.e. we fix them in such a way, that $\vec{\chi}$ is exclusively an emergent spherical wave. To this end we divide the derivative of the boundary condition by the boundary condition and equate the result with the corresponding numerical expression evaluated at an arbitrary but sufficiently large $r = \tilde{r}$,

$$\frac{(d/dr)(r h_1^{(1)}(k_\alpha r))|_{r=\tilde{r}}}{\tilde{r} h_1^{(1)}(k_\alpha \tilde{r})} = \frac{(d/dr)\chi_{\text{numerical},\alpha}(r)|_{r=\tilde{r}}}{\chi_{\text{numerical},\alpha}(\tilde{r})}, \quad \alpha = BB, B^*B^*. \quad (32)$$

These two equations are independent of the still unknown T matrix elements and can be solved with respect to the two coefficients a and b .

- (3) Finally, we determine the T matrix elements $t_{BB;BB}$ and $t_{BB;B^*B^*}$ from $\vec{\chi}_{\text{numerical}}(r)$ via

$$t_{BB;\alpha} = \frac{\chi_{\text{numerical},\alpha}(\tilde{r})}{i\tilde{r} h_1^{(1)}(k_\alpha \tilde{r})}, \quad (33)$$

where we have again used the boundary conditions at $r \rightarrow \infty$, Eq. (29).

The entries in the second row of the T matrix (28), $t_{B^*B^*;BB}$ and $t_{B^*B^*;B^*B^*}$, corresponding to an incident B^*B^* wave, can be determined in the same way. One just has to use coefficients $(A_{BB}, A_{B^*B^*}) = (0, 1)$ and replace the boundary conditions (29) by the boundary conditions (30).

V Numerical Results

V.I Input Parameters and Error Analysis

Unless explicitly stated otherwise, we use for the following numerical analysis a bottom quark mass $m_b = 4977$ MeV taken from a quark model [78] and a meson mass splitting $m_{B^*} - m_B = 45$ MeV as listed by the PDG [73]. Moreover, as discussed in Section II, we use potential parameterizations (5) with parameters $\alpha_5 = 0.34 \pm 0.03$, $d_5 = 0.45_{-0.10}^{+0.12}$ fm, $\alpha_j = -0.10 \pm 0.07$ and $d_j = (0.28 \pm 0.017)$ fm provided in Refs. [53, 55].

Uncertainties of numerical results in this work are estimated by propagation of uncertainties of the potential parameters. For the parameters $\alpha_5 = 0.34 \pm 0.03$, $\alpha_j = -0.10 \pm 0.07$ and $d_j = (0.28 \pm 0.017)$ fm, which have symmetric errors, we assume Gaussian distributions. For the parameter $d_5 = 0.45_{-0.10}^{+0.12}$ fm we assume a skewed normal distribution with a positive skewness with parameters tuned in such a way, that the 16th and 84th percentiles correspond to the lower and upper errors of d_5 . From these distributions we draw 1000 random parameter samples $(\alpha_5, d_5, \alpha_j, d_j)$. Physical quantities like positions of T matrix poles or branching ratios are computed for each of

these samples. For some of these samples the imaginary part of the T matrix pole is rather large and precisely locating the pole is numerically difficult. Moreover, a large imaginary part is equivalent to a large decay width, which implies that it is rather difficult or even impossible to experimentally detect the corresponding resonance. We thus discard all poles with $\text{Im}(E_{\text{pole}}) < -200$ MeV amounting to $\approx 14\%$ of the samples. The uncertainties of pole positions and related quantities are then defined by the 16th and 84th percentiles on the remaining $\approx 86\%$ of the samples.

V.II Mass and Decay Width

V.II.1 Mass and Decay Width for Physical Parameters

A pole of the T matrix in the complex energy plane signals a tetraquark bound state (for $\text{Re}(E_{\text{pole}}) < 2m_B$ and $\text{Im}(E_{\text{pole}}) = 0$) or a tetraquark resonance (for $\text{Re}(E_{\text{pole}}) > 2m_B$ and $\text{Im}(E_{\text{pole}}) < 0$), where E_{pole} denotes the pole position. The corresponding mass is

$$m = \text{Re}(E_{\text{pole}}) \quad (34)$$

and the decay width, in case of a resonance, is

$$\Gamma = -2\text{Im}(E_{\text{pole}}). \quad (35)$$

We compute the T matrix for given energy E as discussed in Section IV.III. To locate possibly existing poles, we first scan the complex energy plane for singularities in $\det(\text{T})$, i.e. for significantly enhanced $|\det(\text{T})|$. This is done by sampling $\det(\text{T})$ on a uniform grid in the region $1 \text{ MeV} \leq \text{Re}(E - 2m_B) \leq 120 \text{ MeV}$ and $-100 \text{ MeV} \leq \text{Im}(E - 2m_B) \leq -1 \text{ MeV}$ with spacing 1 MeV in both real and imaginary direction. When a singularity is indicated, we determine the corresponding pole position precisely by computing the nearby root of $1/\det(\text{T})$. For that we use Newton's method with an initial guess for E provided by the energy scan.

For physical parameters, i.e. for physical bottom quark mass, meson mass splitting and potential parametrizations as listed in Section V.I, we find a pole with corresponding resonance mass and decay width

$$m = 2m_B + 94.0_{-5.4}^{+1.3} = 2m_{B^*} + 4.0_{-5.4}^{+1.3} \text{ MeV} \quad , \quad \Gamma = 140_{-66}^{+86} \text{ MeV}. \quad (36)$$

This pole is illustrated in Figure 2, where $|\det(\text{T})|$ is plotted as a function of the complex energy E .

At first glance this result is surprising, because in our previous work [71], based on a single-channel Schrödinger equation with heavy spin effects neglected, we predicted a resonance with mass $m_{\text{single-channel}} = 2m_B + 17_{-4}^{+4}$ MeV slightly above the BB threshold. Now, with our refined coupled-channel approach, the resonance mass is significantly larger, $m = 2m_B + 94.0_{-5.4}^{+1.3}$ MeV, i.e. slightly above the B^*B^* threshold. This drastic shift in the resonance mass, when including heavy spin effects, is a direct consequence of the structure of the coupled-channel Schrödinger equation (26) and can be understood as follows.

The upper component of the 2-component wave function $\vec{\chi} = (\chi_{BB}, \chi_{B^*B^*})^T$ represents the BB channel and the lower component the B^*B^* channel, as indicated by the diagonal mass matrix $\text{diag}(2m_B, 2m_{B^*})$ in Eq. (26). Heavy spin effects are caused on the one hand by the mass splitting $m_{B^*} - m_B = 45$ MeV and on the other hand by the 2×2 potential matrix (16). The relevant potential for BB is $(V_5(r) + 3V_j(r))/4$ (the upper left entry of the potential matrix (16)). The attractive contribution $V_5(r)$ is suppressed by the factor 1/4 and there is an additional compensation of the attraction by the repulsive $V_j(r)$, which is enhanced by a relative factor of 3. As a consequence, the net attractive force is negligible and a BB resonance cannot be expected. In contrast to that, the relevant potential for B^*B^* is $(3V_5(r) + V_j(r))/4$ (the lower right entry of the potential matrix (16)). This time, the attractive contribution $V_5(r)$ is only weakly suppressed by the factor 3/4 and there is essentially no additional compensation of the attraction by the anyway rather weak repulsive $V_j(r)$. Consequently, a resonance with a sizable B^*B^* component close to the B^*B^* can be expected and is numerically found (see Eq. (36) and the discussion of branching ratios in Section V.III).

We note that an $I(J^P) = 0(1^-) \bar{b}b u d$ tetraquark resonances was also predicted recently using a constituent quark model [26]. The result from that reference, $m_{[26]} = 10762(3) \text{ MeV} \approx 2m_B + 200 \text{ MeV}$, is larger than our lattice QCD-based result, but still in crude qualitative agreement.

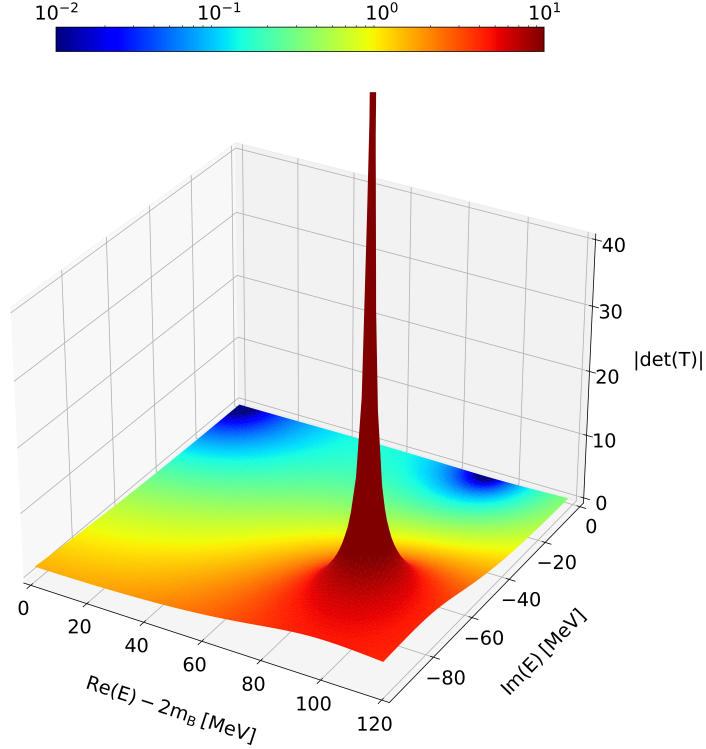


Figure 2: $|\det(T)|$ as function of the complex energy.

V.II.2 Varying the relative weights of $V_5(r)$ and $V_j(r)$ with respect to the BB and the B^*B^* Channel

The 2×2 potential matrix (16) leads to a coupling of the BB and the B^*B^* channel. To better understand the significant difference in the resonance mass, when comparing the coupled-channel result (36) of this work to the single-channel result from Ref. [71], we introduce an additional parameter $0 \leq \theta \leq \pi/2$ in the potential matrix (16),

$$\begin{aligned}
 H_{\text{int},S=0} &\rightarrow H_{\text{int},S=0}(\theta) = R^T(\theta) \begin{pmatrix} V_5(r) & 0 \\ 0 & V_j(r) \end{pmatrix} R(\theta) = \\
 &= \begin{pmatrix} \cos^2 \theta V_5(r) + \sin^2 \theta V_j(r) & \sin \theta \cos \theta (V_5(r) - V_j(r)) \\ \sin \theta \cos \theta (V_5(r) - V_j(r)) & \sin^2 \theta V_5(r) + \cos^2 \theta V_j(r) \end{pmatrix}, \quad (37)
 \end{aligned}$$

where $R(\theta)$ is an ordinary rotation matrix,

$$R(\theta) = \begin{pmatrix} +\cos \theta & +\sin \theta \\ -\sin \theta & +\cos \theta \end{pmatrix}. \quad (38)$$

For $\theta = 0$ the Schrödinger equation decouples into two independent equations, where the upper BB equation is identical to the single-channel equation studied in Ref. [71]. $\theta = \pi/3$ corresponds to the coupled-channel equation (26) derived in Section IV and solved in Section V.II.1, i.e. $H_{\text{int},S=0}(\theta = \pi/3)$ is identical to the potential matrix (16). For $\theta = \pi/2$ the Schrödinger equation decouples again into two independent equations, where this time the lower B^*B^* equation is identical to the single-channel equation from Ref. [71] with exception of a constant energy shift by $2(m_{B^*} - m_B) = 90$ MeV. The parameter θ , thus, allows to continuously rotate the attractive potential $V_5(r)$ from the BB channel to the B^*B^* channel and vice versa for the repulsive potential $V_j(r)$.

In Figure 3 we explore the effect of this rotation, i.e. we show the trajectory of the T matrix pole in the complex energy plane, when changing θ from 0 to $\pi/2$. For $\theta = 0$ as well as for $\theta = \pi/2$ the result from Ref. [71] is reproduced

², in the latter case shifted by $2(m_{B^*} - m_B)$ as discussed in the previous paragraph. It is, thus, not surprising that the resonance mass monotonically increases from $m \approx 2m_B + 18 \text{ MeV}$ at $\theta = 0$ to $m \approx 2m_B + 108 \text{ MeV} = 2m_{B^*} + 18 \text{ MeV}$ at $\theta = \pi/2$. At the physical point corresponding to $\theta = \pi/3$ the attractive potential is split between the BB and the B^*B^* channel in a 1:3 ratio, i.e. there is a sizable attraction between two B^* mesons, but essentially no attraction between two B mesons. This explains the location of the resonance mass (36) close to the B^*B^* threshold, as already discussed at the end of Section V.II.1.

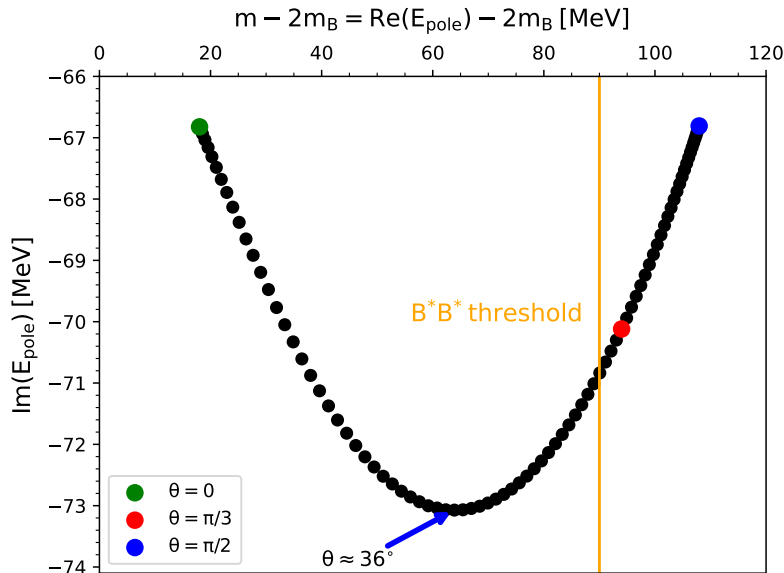


Figure 3: Trajectory of the T matrix pole in the complex energy plane, when changing θ from 0 to $\pi/2$.

V.II.3 Varying the Heavy Quark Mass

For sufficiently large heavy quark mass, the resonance found in Section V.II.1 should turn into a bound state. We explore this by replacing

$$m_b \rightarrow \kappa m_b \quad (39)$$

and continuously increasing κ , starting from $\kappa = 1$. We note that the meson mass difference $\Delta m = m_{B^*} - m_B$ strongly depends on the heavy quark mass, as can e.g. be seen by comparing experimentally known masses of the charm mesons D and D^* and of the bottom mesons B and B^* . To account for this dependence, we use the leading order result from Heavy Quark Effective Theory [79–81],

$$\Delta m = \frac{m_{B^*} - m_B}{\kappa} = \frac{45 \text{ MeV}}{\kappa}. \quad (40)$$

In Figure 4 we show $m - 2m_B = \text{Re}(E_{\text{pole}}) - 2m_B$ as function of κ . When increasing κ , starting from $\kappa = 1$, the resonance moves closer to the BB threshold, until at $\kappa \approx 2.82$ it becomes a bound state. The dependence of the resonance or bound state mass on κ exhibits an almost linear behavior.

In Figure 5 we visualize, how the existence of a resonance or bound state depends on θ (i.e. the splitting of the potentials $V_5(r)$ and $V_j(r)$ between the BB and the B^*B^* channel) and on κ (i.e. the heavy quark mass). The black dots (connected by straight red lines to guide the eye) separate a resonance (blue region) from a bound state (green region).

²In the single channel case we find the resonance mass 18 MeV above threshold, i.e. there is a tiny difference to the 17 MeV quoted in Ref. [71]. The reason is that we use the b quark mass in the kinetic term of the Schrödinger equation, while in Ref. [71] the B meson mass was used.

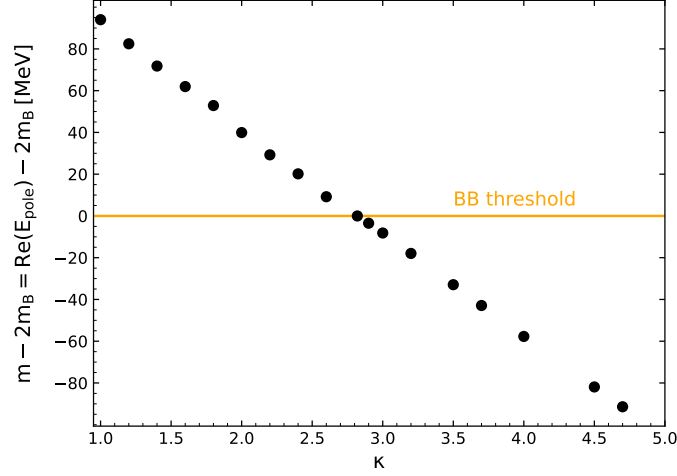


Figure 4: $m - 2m_B = \text{Re}(E_{\text{pole}}) - 2m_B$ as function of κ .

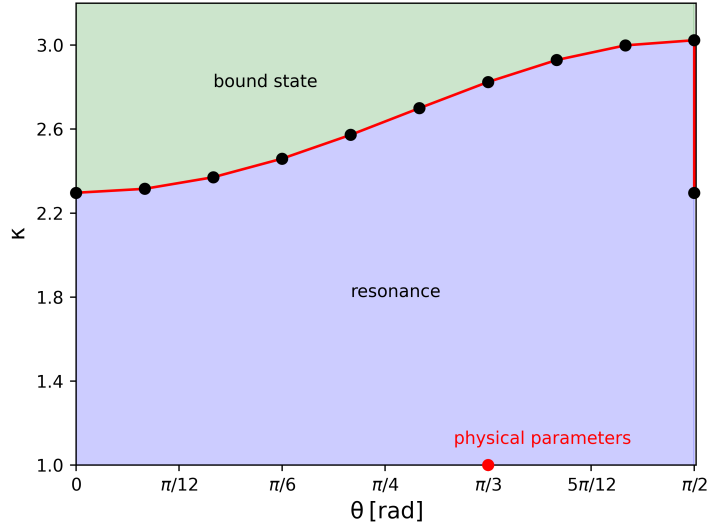


Figure 5: Existence of a resonance or bound state in the θ - κ plane (see Section V.II.2 and Section V.II.3 for detailed explanations of these parameters). Note that at $\theta = \pi/2$ there is a discontinuity in the curve separating the two regions, because the 2×2 Schrödinger equation decouples into two independent equations and the lowest threshold suddenly changes from $2m_B$ to $2m_{B^*}$.

V.III Branching Ratios

In addition to the mass and the decay width of the $I(J^P) = 0(1^-) \bar{b}\bar{b}ud$ tetraquark resonance, it is also of interest to study its decay channels. The resonance can decay into a BB meson pair or into a B^*B^* meson pair. In experiments decay probabilities to different channels α are referred to as branching ratios BR_α . Theoretically, branching ratios can be approximated by the residues of the diagonal entries of the T matrix at the pole energy (see e.g. Ref. [82]), in our case

$$\text{BR}_\alpha = \frac{|\text{Res}(t_{\alpha;\alpha})|}{|\text{Res}(t_{BB;BB})| + |\text{Res}(t_{B^*B^*;B^*B^*})|}, \quad \alpha = BB, B^*B^*. \quad (41)$$

To compute the residues we use the residue theorem

$$\text{Res}(t_{\alpha;\alpha}) = \frac{1}{2\pi i} \oint_{\mathcal{C}} dE t_{\alpha;\alpha}(E), \quad (42)$$

where \mathcal{C} is a closed contour in the complex energy plane encircling the T matrix pole at position E_{pole} . We choose a circle with radius $r = 1 \text{ MeV}$ around the pole as contour \mathcal{C} parameterized by

$$E(\lambda) = E_{\text{pole}} + r e^{2\pi i \lambda} \quad (43)$$

with $0 \leq \lambda \leq 1$. The integral (42) can be solved numerically in a straightforward way. We verified the stability of the resulting residues and branching ratios by varying the number of integration points and the radius r .

In Figure 6 we show the branching ratios BR_{BB} and $\text{BR}_{B^*B^*} = 1 - \text{BR}_{BB}$ as functions of the angle θ defined in Section V.II.2. For the physical value $\theta = \pi/3$ we find

$$\text{BR}_{BB} = 26_{-4}^{+9}\% \quad , \quad \text{BR}_{B^*B^*} = 74_{-9}^{+4}\% \quad (44)$$

indicating a significantly favored decay of the tetraquark resonance to B^*B^* . This is consistent with our results from Section V.II.1, where we found a resonance mass close to the B^*B^* threshold suggesting that the resonance is mainly composed of a B^*B^* pair and that $\text{BR}_{B^*B^*} \gg \text{BR}_{BB}$.

Decreasing the angle θ shifts the attractive potential $V_5(r)$ towards the BB channel, which is reflected in an increasing branching ratio BR_{BB} . At $\theta = 0$ the Schrödinger equation (26) decouples into a BB and a B^*B^* equation, as discussed in Section V.II.2. The resonance is then obtained from the BB equation (which was already studied in Ref. [71]) and, consequently, $\text{BR}_{BB} = 100\%$. Similarly, increasing the angle θ shifts the attractive potential $V_5(r)$ towards the B^*B^* channel, leading to an increasing branching ratio $\text{BR}_{B^*B^*}$, where $\text{BR}_{B^*B^*} = 100\%$ at $\theta = \pi/2$.

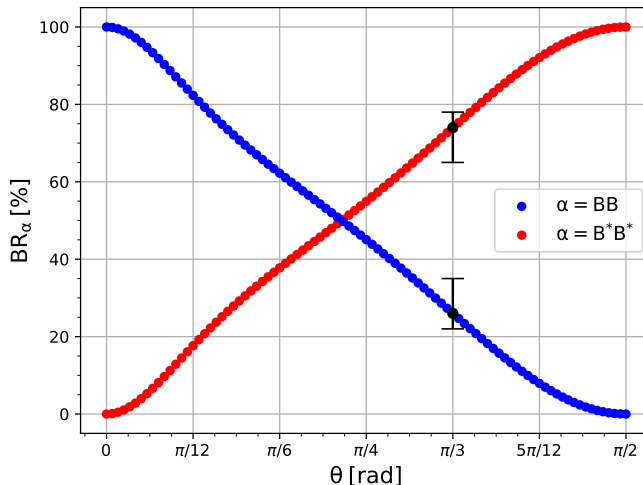


Figure 6: Branching ratios BR_{BB} and $\text{BR}_{B^*B^*} = 1 - \text{BR}_{BB}$ as functions of the angle θ defined in Section V.II.2.

VI Conclusions and Outlook

In this work we predicted a $\bar{b}b u d$ tetraquark resonance with quantum numbers $I(J^P) = 0(1^-)$ slightly above the B^*B^* threshold using antistatic-antistatic potentials computed with lattice QCD and the Born-Oppenheimer approximation. The mass and decay width of this resonance are $m = 2m_B + 94.0_{-5.4}^{+1.3} \text{ MeV} = 2m_{B^*} + 4.0_{-5.4}^{+1.3} \text{ MeV}$ and $\Gamma = 140_{-66}^{+86} \text{ MeV}$. On a technical level, we significantly refined our single-channel approach from Ref. [71], where we did not distinguish between B and B^* mesons, which are degenerate in the static limit. Now we incorporated their mass difference of around 45 MeV by setting up a coupled-channel Schrödinger equation containing not only an attractive potential $V_5(r)$ (already used in Ref. [71]), but also a repulsive potential $V_j(r)$.

In addition to the numerical prediction of the mass and decay width, our formalism also led to a solid physical understanding, why there is a $\bar{b}bud$ tetraquark resonance close to the B^*B^* threshold, but not in the region of the BB threshold, as naively expected from our previous work [71]. The reason is that the attractive potential $V_5(r)$ dominates the B^*B^* channel, but is strongly suppressed in the BB channel, whereas the situation is reversed for the repulsive potential $V_j(r)$. This theoretical result is consistent with and supported by further numerical results on branching ratios, which indicate that a decay of the $I(J^P) = 0(1^-)$ $\bar{b}bud$ tetraquark resonance is around three times more likely to a B^*B^* pair than to a BB pair.

The Born-Oppenheimer approach and the antistatic-antistatic lattice QCD potentials, on which our work is based, introduce systematic errors, which are difficult to quantify precisely. As a crude estimate we compare results obtained for a related QCD-stable $\bar{b}bud$ tetraquark with quantum numbers $I(J^P) = 0(1^+)$. The Born-Oppenheimer approach using the same lattice QCD potentials and the same formalism to derive a coupled-channel Schrödinger equation leads to a binding energy of 59^{+30}_{-38} MeV [55]. This binding energy has, meanwhile, been computed within full lattice QCD by several independent groups, where their results point towards a binding energy around 100 MeV [56–58, 60, 63, 64, 67]. In view of this comparison it seems likely that an $I(J^P) = 0(1^-)$ $\bar{b}bud$ tetraquark resonance exists, since the Born-Oppenheimer approach with the used potentials leads to results in fair agreement with full lattice QCD predictions, even having a slight tendency of underestimating the binding.

This work is also intended as an exploratory and preparatory investigation for a future full lattice QCD investigation of the predicted $I(J^P) = 0(1^-)$ $\bar{b}bud$ tetraquark resonance. The most important findings and main takeaways for such a full lattice QCD investigation are the following:

- (i) The existence of a tetraquark resonance can be expected close to the B^*B^* threshold, i.e. significantly above the BB threshold.
- (ii) Because of (i) and since the $\bar{b}bud$ tetraquark resonance predominantly decays to a B^*B^* pair, it will be imperative to use scattering interpolating operators of both BB and B^*B^* type, to reliably extract finite volume energy levels up to the region of the B^*B^* threshold.
- (iii) Because of (i) and (ii), a standard single-channel scattering analysis of finite volume energy levels is not sufficient. One rather has to resort to technically more difficult coupled-channel finite volume scattering techniques (see e.g. Ref. [83]).

In recent work we have prepared and tested a lattice QCD setup with $\bar{b}bud$ scattering operators both at the source and at the sink of correlation functions [67]. This setup is perfectly suited for an implementation of the BB and B^*B^* scattering operators mentioned in (ii). We plan to continue our work in this direction in the near future with the main goal to arrive at a rigorous full lattice QCD prediction of the $I(J^P) = 0(1^-)$ $\bar{b}bud$ tetraquark resonance using finite-volume methods as referenced in (iii).

Acknowledgements

We thank André Zimmermann-Santos for collaboration on earlier related work. We acknowledge useful discussions with Pedro Bicudo, Lasse Müller and Martin Pflaumer.

J.H. acknowledges support by a “Rolf and Edith Sandvoss Stipendium”. M.W. acknowledges support by the Deutsche Forschungsgemeinschaft (DFG, German Research Foundation) – project number 457742095. M.W. acknowledges support by the Heisenberg Programme of the Deutsche Forschungsgemeinschaft (DFG, German Research Foundation) – project number 399217702.

Calculations on the GOETHE-NHR and on the FUCHS-CSC high-performance computers of the Frankfurt University were conducted for this research. We would like to thank HPC-Hessen, funded by the State Ministry of Higher Education, Research and the Arts, for programming advice.

References

- [1] R. J. Jaffe, “Multi-quark hadrons. i. phenomenology of $Q^2\bar{q}^2$ mesons,” *Phys. Rev. D* **15** (Jan, 1977) 267–280. <https://link.aps.org/doi/10.1103/PhysRevD.15.267>.

- [2] Belle Collaboration, A. Bondar *et al.*, “Observation of two charged bottomonium-like resonances in $Y(5S)$ decays,” *Phys. Rev. Lett.* **108** (2012) 122001, [arXiv:1110.2251 \[hep-ex\]](#).
- [3] T. Xiao, S. Dobbs, A. Tomaradze, and K. K. Seth, “Observation of the Charged Hadron $Z_c^\pm(3900)$ and Evidence for the Neutral $Z_c^0(3900)$ in $e^+e^- \rightarrow \pi\pi J/\psi$ at $\sqrt{s} = 4170$ MeV,” *Phys. Lett. B* **727** (2013) 366–370, [arXiv:1304.3036 \[hep-ex\]](#).
- [4] LHCb Collaboration, R. Aaij *et al.*, “Observation of the resonant character of the $Z(4430)^-$ state,” *Phys. Rev. Lett.* **112** no. 22, (2014) 222002, [arXiv:1404.1903 \[hep-ex\]](#).
- [5] BESIII Collaboration, M. Ablikim *et al.*, “Observation of a Charged Charmoniumlike Structure $Z_c(4020)$ and Search for the $Z_c(3900)$ in $e^+e^- \rightarrow \pi^+\pi^-h_c$,” *Phys. Rev. Lett.* **111** no. 24, (2013) 242001, [arXiv:1309.1896 \[hep-ex\]](#).
- [6] LHCb Collaboration, R. Aaij *et al.*, “Model-independent confirmation of the $Z(4430)^-$ state,” *Phys. Rev. D* **92** no. 11, (2015) 112009, [arXiv:1510.01951 \[hep-ex\]](#).
- [7] BESIII Collaboration, M. Ablikim *et al.*, “Confirmation of a charged charmoniumlike state $Z_c(3885)^\mp$ in $e^+e^- \rightarrow \pi^\pm(DD^*)^\mp$ with double D tag,” *Phys. Rev. D* **92** no. 9, (2015) 092006, [arXiv:1509.01398 \[hep-ex\]](#).
- [8] LHCb Collaboration, R. Aaij *et al.*, “Observation of an exotic narrow doubly charmed tetraquark,” *Nature Phys.* **18** no. 7, (2022) 751–754, [arXiv:2109.01038 \[hep-ex\]](#).
- [9] J. Carlson, L. Heller, and J. A. Tjon, “Stability of Dimesons,” *Phys. Rev. D* **37** (1988) 744.
- [10] A. V. Manohar and M. B. Wise, “Exotic $QQ\bar{q}\bar{q}$ states in QCD,” *Nucl. Phys. B* **399** (1993) 17–33, [arXiv:hep-ph/9212236](#).
- [11] C.-K. Chow, “Semileptonic decays of heavy tetraquarks,” *Phys. Rev. D* **51** (1995) 3541–3543, [arXiv:hep-ph/9411221](#).
- [12] D. M. Brink and F. Stancu, “Tetraquarks with heavy flavors,” *Phys. Rev. D* **57** (1998) 6778–6787.
- [13] J. Vijande, F. Fernandez, A. Valcarce, and B. Silvestre-Brac, “Tetraquarks in a chiral constituent quark model,” *Eur. Phys. J. A* **19** (2004) 383, [arXiv:hep-ph/0310007](#).
- [14] J. Vijande, A. Valcarce, and K. Tsushima, “Dynamical study of $QQ\bar{u}\bar{d}$ mesons,” *Phys. Rev. D* **74** (2006) 054018, [arXiv:hep-ph/0608316](#).
- [15] D. Ebert, R. N. Faustov, V. O. Galkin, and W. Lucha, “Masses of tetraquarks with two heavy quarks in the relativistic quark model,” *Phys. Rev. D* **76** (2007) 114015, [arXiv:0706.3853 \[hep-ph\]](#).
- [16] M. Zhang, H. X. Zhang, and Z. Y. Zhang, “ $QQ\bar{q}\bar{q}$ four-quark bound states in chiral SU(3) quark model,” *Commun. Theor. Phys.* **50** (2008) 437–440, [arXiv:0711.1029 \[nucl-th\]](#).
- [17] H. J. Lipkin, “Exotic hadrons in the constituent quark model,” *Prog. Theor. Phys. Suppl.* **168** (2007) 15–22, [arXiv:hep-ph/0703190](#).
- [18] S. Godfrey and S. L. Olsen, “The Exotic XYZ Charmonium-like Mesons,” *Ann. Rev. Nucl. Part. Sci.* **58** (2008) 51–73, [arXiv:0801.3867 \[hep-ph\]](#).
- [19] S. H. Lee and S. Yasui, “Stable multi-quark states with heavy quarks in a diquark model,” *Eur. Phys. J. C* **64** (2009) 283–295, [arXiv:0901.2977 \[hep-ph\]](#).
- [20] M. Karliner and S. Nussinov, “The doubly heavies: $\bar{Q}Q\bar{q}q$ and $QQ\bar{Q}\bar{q}$ tetraquarks and QQq baryons,” *JHEP* **07** (2013) 153, [arXiv:1304.0345 \[hep-ph\]](#).
- [21] P. Bicudo and M. Cardoso, “Tetraquark bound states and resonances in the unitary and microscopic triple string flip-flop quark model, the light-light-antiheavy-antiheavy $qq\bar{Q}\bar{Q}$ case study,” *Phys. Rev. D* **94** no. 9, (2016) 094032, [arXiv:1509.04943 \[hep-ph\]](#).

- [22] M. Karliner and J. L. Rosner, “Discovery of doubly-charmed Ξ_{cc} baryon implies a stable $(bb\bar{u}\bar{d})$ tetraquark,” *Phys. Rev. Lett.* **119** no. 20, (2017) 202001, [arXiv:1707.07666 \[hep-ph\]](#).
- [23] E. J. Eichten and C. Quigg, “Heavy-quark symmetry implies stable heavy tetraquark mesons $Q_i Q_j \bar{q}_k \bar{q}_l$,” *Phys. Rev. Lett.* **119** no. 20, (2017) 202002, [arXiv:1707.09575 \[hep-ph\]](#).
- [24] W. Park, S. Noh, and S. H. Lee, “Masses of the doubly heavy tetraquarks in a constituent quark model,” *Nucl. Phys. A* **983** (2019) 1–19, [arXiv:1809.05257 \[nucl-th\]](#).
- [25] J.-M. Richard, A. Valcarce, and J. Vijande, “Few-body quark dynamics for doubly heavy baryons and tetraquarks,” *Phys. Rev. C* **97** no. 3, (2018) 035211, [arXiv:1803.06155 \[hep-ph\]](#).
- [26] Q. Meng, M. Harada, E. Hiyama, A. Hosaka, and M. Oka, “Doubly heavy tetraquark resonant states,” *Phys. Lett. B* **824** (2022) 136800, [arXiv:2106.11868 \[hep-ph\]](#).
- [27] T. Guo, J. Li, J. Zhao, and L. He, “Mass spectra of doubly heavy tetraquarks in an improved chromomagnetic interaction model,” *Phys. Rev. D* **105** no. 1, (2022) 014021, [arXiv:2108.10462 \[hep-ph\]](#).
- [28] J.-M. Richard, A. Valcarce, and J. Vijande, “Doubly-heavy tetraquark bound states and resonances,” *Nucl. Part. Phys. Proc.* **324-329** (2023) 64–67, [arXiv:2209.07372 \[hep-ph\]](#).
- [29] P. G. Ortega, D. R. Entem, and F. Fernández, “Exploring $T_{\psi\psi}$ tetraquark candidates in a coupled-channels formalism,” *Phys. Rev. D* **108** no. 9, (2023) 094023, [arXiv:2307.00532 \[hep-ph\]](#).
- [30] X.-Y. Liu, W.-X. Zhang, and D. Jia, “Doubly heavy tetraquarks: Heavy quark bindings and chromomagnetically mixings,” *Phys. Rev. D* **108** no. 5, (2023) 054019, [arXiv:2303.03923 \[hep-ph\]](#).
- [31] R. D. Matheus and M. Nielsen, “X(3872) as tetraquarks in QCD sum rules,” *Int. J. Mod. Phys. E* **16** (2007) 2906–2909.
- [32] F. S. Navarra, M. Nielsen, and S. H. Lee, “QCD sum rules study of $QQ\bar{u}\bar{d}$ mesons,” *Phys. Lett. B* **649** (2007) 166–172, [arXiv:hep-ph/0703071](#).
- [33] W. Chen, T. G. Steele, and S.-L. Zhu, “Exotic open-flavor $bc\bar{q}\bar{q}$, $bc\bar{s}\bar{s}$ and $qc\bar{q}\bar{b}$, $sc\bar{s}\bar{b}$ tetraquark states,” *Phys. Rev. D* **89** no. 5, (2014) 054037, [arXiv:1310.8337 \[hep-ph\]](#).
- [34] Z.-G. Wang, “Analysis of the axialvector doubly heavy tetraquark states with QCD sum rules,” *Acta Phys. Polon. B* **49** (2018) 1781, [arXiv:1708.04545 \[hep-ph\]](#).
- [35] S. S. Agaev, K. Azizi, and H. Sundu, “Open charm-bottom scalar tetraquarks and their strong decays,” *Phys. Rev. D* **95** no. 3, (2017) 034008, [arXiv:1611.00293 \[hep-ph\]](#).
- [36] L. Tang, B.-D. Wan, K. Maltman, and C.-F. Qiao, “Doubly Heavy Tetraquarks in QCD Sum Rules,” *Phys. Rev. D* **101** no. 9, (2020) 094032, [arXiv:1911.10951 \[hep-ph\]](#).
- [37] S. S. Agaev, K. Azizi, B. Barsbay, and H. Sundu, “Stable scalar tetraquark $T_{bb;\bar{u}\bar{d}}^-$,” *Eur. Phys. J. A* **56** (2020) 177, [arXiv:2001.01446 \[hep-ph\]](#).
- [38] S. S. Agaev, K. Azizi, and H. Sundu, “Newly observed exotic doubly charmed meson T_{cc}^+ ,” *Nucl. Phys. B* **975** (2022) 115650, [arXiv:2108.00188 \[hep-ph\]](#).
- [39] S. Ohkoda, Y. Yamaguchi, S. Yasui, K. Sudoh, and A. Hosaka, “Exotic mesons with double charm and bottom flavor,” *Phys. Rev. D* **86** (2012) 034019, [arXiv:1202.0760 \[hep-ph\]](#).
- [40] E. Braaten, C. Langmack, and D. H. Smith, “Born-Oppenheimer Approximation for the XYZ Mesons,” *Phys. Rev. D* **90** no. 1, (2014) 014044, [arXiv:1402.0438 \[hep-ph\]](#).
- [41] J. Segovia, “Effective field theory investigations of the XYZ puzzle,” *J. Phys. Conf. Ser.* **742** no. 1, (2016) 012005, [arXiv:1603.08527 \[hep-ph\]](#).
- [42] J. Soto and J. Tarrús Castellà, “Nonrelativistic effective field theory for heavy exotic hadrons,” *Phys. Rev. D* **102** no. 1, (2020) 014012, [arXiv:2005.00552 \[hep-ph\]](#).

- [43] E. Braaten, L.-P. He, and A. Mohapatra, “Masses of doubly heavy tetraquarks with error bars,” *Phys. Rev. D* **103** no. 1, (2021) 016001, [arXiv:2006.08650 \[hep-ph\]](#).
- [44] L. Maiani, A. Pilloni, A. D. Polosa, and V. Riquer, “Doubly heavy tetraquarks in the Born-Oppenheimer approximation,” *Phys. Lett. B* **836** (2023) 137624, [arXiv:2208.02730 \[hep-ph\]](#).
- [45] M. Berwein, N. Brambilla, A. Mohapatra, and A. Vairo, “Hybrids, tetraquarks, pentaquarks, doubly heavy baryons, and quarkonia in Born-Oppenheimer effective theory,” *Phys. Rev. D* **110** no. 9, (2024) 094040, [arXiv:2408.04719 \[hep-ph\]](#).
- [46] W. Heupel, G. Eichmann, and C. S. Fischer, “Tetraquark Bound States in a Bethe-Salpeter Approach,” *Phys. Lett. B* **718** (2012) 545–549, [arXiv:1206.5129 \[hep-ph\]](#).
- [47] N. Santowsky and C. S. Fischer, “Four-quark states with charm quarks in a two-body Bethe-Salpeter approach,” *Eur. Phys. J. C* **82** no. 4, (2022) 313, [arXiv:2111.15310 \[hep-ph\]](#).
- [48] J. Hoffer, G. Eichmann, and C. S. Fischer, “The structure of open-flavour four-quark states in the charm and bottom region,” [arXiv:2409.05779 \[hep-ph\]](#).
- [49] **NPLQCD** Collaboration, W. Detmold, K. Orginos, and M. J. Savage, “ BB potentials in quenched lattice QCD,” *Phys. Rev. D* **76** (2007) 114503, [arXiv:hep-lat/0703009](#).
- [50] **ETM** Collaboration, M. Wagner, “Forces between static-light mesons,” *PoS LATTICE2010* (2010) 162, [arXiv:1008.1538 \[hep-lat\]](#).
- [51] **QCDSF** Collaboration, G. Bali and M. Hetzenegger, “Potentials between pairs of static-light mesons,” *PoS LATTICE2011* (2011) 123, [arXiv:1111.2222 \[hep-lat\]](#).
- [52] Z. S. Brown and K. Orginos, “Tetraquark bound states in the heavy-light heavy-light system,” *Phys. Rev. D* **86** (2012) 114506, [arXiv:1210.1953 \[hep-lat\]](#).
- [53] P. Bicudo, K. Cichy, A. Peters, and M. Wagner, “ BB interactions with static bottom quarks from Lattice QCD,” *Phys. Rev. D* **93** no. 3, (2016) 034501, [arXiv:1510.03441 \[hep-lat\]](#).
- [54] **European Twisted Mass** Collaboration, P. Bicudo and M. Wagner, “Lattice QCD signal for a bottom-bottom tetraquark,” *Phys. Rev. D* **87** no. 11, (2013) 114511, [arXiv:1209.6274 \[hep-ph\]](#).
- [55] P. Bicudo, J. Scheunert, and M. Wagner, “Including heavy spin effects in the prediction of a $\bar{b}b\bar{u}d$ tetraquark with lattice QCD potentials,” *Phys. Rev. D* **95** no. 3, (2017) 034502, [arXiv:1612.02758 \[hep-lat\]](#).
- [56] A. Francis, R. J. Hudspith, R. Lewis, and K. Maltman, “Lattice Prediction for Deeply Bound Doubly Heavy Tetraquarks,” *Phys. Rev. Lett.* **118** no. 14, (2017) 142001, [arXiv:1607.05214 \[hep-lat\]](#).
- [57] P. Junnarkar, N. Mathur, and M. Padmanath, “Study of doubly heavy tetraquarks in Lattice QCD,” *Phys. Rev. D* **99** no. 3, (2019) 034507, [arXiv:1810.12285 \[hep-lat\]](#).
- [58] L. Leskovec, S. Meinel, M. Pflaumer, and M. Wagner, “Lattice QCD investigation of a doubly-bottom $\bar{b}b\bar{u}d$ tetraquark with quantum numbers $I(J^P) = 0(1^+)$,” *Phys. Rev. D* **100** no. 1, (2019) 014503, [arXiv:1904.04197 \[hep-lat\]](#).
- [59] R. J. Hudspith, B. Colquhoun, A. Francis, R. Lewis, and K. Maltman, “A lattice investigation of exotic tetraquark channels,” *Phys. Rev. D* **102** (2020) 114506, [arXiv:2006.14294 \[hep-lat\]](#).
- [60] P. Mohanta and S. Basak, “Construction of $bb\bar{u}\bar{d}$ tetraquark states on lattice with NRQCD bottom and HISQ up and down quarks,” *Phys. Rev. D* **102** no. 9, (2020) 094516, [arXiv:2008.11146 \[hep-lat\]](#).
- [61] M. Padmanath and S. Prelovsek, “Signature of a Doubly Charm Tetraquark Pole in DD^* Scattering on the Lattice,” *Phys. Rev. Lett.* **129** no. 3, (2022) 032002, [arXiv:2202.10110 \[hep-lat\]](#).
- [62] S. Meinel, M. Pflaumer, and M. Wagner, “Search for $\bar{b}b\bar{u}s$ and $\bar{b}b\bar{u}d$ tetraquark bound states using lattice QCD,” *Phys. Rev. D* **106** no. 3, (2022) 034507, [arXiv:2205.13982 \[hep-lat\]](#).

- [63] R. J. Hudspith and D. Mohler, “Exotic tetraquark states with two \bar{b} -quarks and $J^P = 0^+$ and 1^+ B_s states in a nonperturbatively tuned lattice NRQCD setup,” *Phys. Rev. D* **107** no. 11, (2023) 114510, [arXiv:2303.17295 \[hep-lat\]](#).
- [64] T. Aoki, S. Aoki, and T. Inoue, “Lattice study on a tetraquark state T_{bb} in the HAL QCD method,” *Phys. Rev. D* **108** no. 5, (2023) 054502, [arXiv:2306.03565 \[hep-lat\]](#).
- [65] M. Padmanath, A. Radhakrishnan, and N. Mathur, “Bound Isoscalar Axial-Vector $bc\bar{u}\bar{d}$ Tetraquark T_{bc} from Lattice QCD Using Two-Meson and Diquark-Antidiquark Variational Basis,” *Phys. Rev. Lett.* **132** no. 20, (2024) 201902, [arXiv:2307.14128 \[hep-lat\]](#).
- [66] C. Alexandrou, J. Finkenrath, T. Leontiou, S. Meinel, M. Pflaumer, and M. Wagner, “Shallow Bound States and Hints for Broad Resonances with Quark Content $\bar{b}\bar{c}ud$ in $B - \bar{D}$ and $B^* - \bar{D}$ Scattering from Lattice QCD,” *Phys. Rev. Lett.* **132** no. 15, (2024) 151902, [arXiv:2312.02925 \[hep-lat\]](#).
- [67] C. Alexandrou, J. Finkenrath, T. Leontiou, S. Meinel, M. Pflaumer, and M. Wagner, “ $\bar{b}\bar{b}ud$ and $\bar{b}\bar{b}us$ tetraquarks from lattice QCD using symmetric correlation matrices with both local and scattering interpolating operators,” [arXiv:2404.03588 \[hep-lat\]](#).
- [68] A. Radhakrishnan, M. Padmanath, and N. Mathur, “Study of the isoscalar scalar $bc\bar{u}\bar{d}$ tetraquark T_{bc} with lattice QCD,” *Phys. Rev. D* **110** no. 3, (2024) 034506, [arXiv:2404.08109 \[hep-lat\]](#).
- [69] S. Collins, A. Nefediev, M. Padmanath, and S. Prelovsek, “Toward the quark mass dependence of T_{cc}^+ from lattice QCD,” *Phys. Rev. D* **109** no. 9, (2024) 094509, [arXiv:2402.14715 \[hep-lat\]](#).
- [70] T. Whyte, D. J. Wilson, and C. E. Thomas, “Near-threshold states in coupled $DD^* - D^*D^*$ scattering from lattice QCD,” [arXiv:2405.15741 \[hep-lat\]](#).
- [71] P. Bicudo, M. Cardoso, A. Peters, M. Pflaumer, and M. Wagner, “ $ud\bar{b}\bar{b}$ tetraquark resonances with lattice QCD potentials and the Born-Oppenheimer approximation,” *Phys. Rev. D* **96** no. 5, (2017) 054510, [arXiv:1704.02383 \[hep-lat\]](#).
- [72] J. Hoffmann, A. Zimmermann-Santos, and M. Wagner, “Inclusion of heavy spin effects in the $ud\bar{b}\bar{b}$ $I(J^P)=0(1^-)$ four-quark channel in the Born-Oppenheimer approximation,” *PoS LATTICE2022* (2023) 262, [arXiv:2211.15765 \[hep-lat\]](#).
- [73] **Particle Data Group** Collaboration, S. Navas *et al.*, “Review of particle physics,” *Phys. Rev. D* **110** no. 3, (2024) 030001.
- [74] P. Bicudo, M. Krstic Marinkovic, L. Müller, and M. Wagner, “Antistatic-antistatic $\bar{Q}\bar{Q}qq$ potentials for u, d and s light quarks from lattice QCD,” in *41st International Symposium on Lattice Field Theory*. 9, 2024. [arXiv:2409.10786 \[hep-lat\]](#).
- [75] P. Bicudo, M. Cardoso, N. Cardoso, and M. Wagner, “Bottomonium resonances with $I = 0$ from lattice QCD correlation functions with static and light quarks,” *Phys. Rev. D* **101** no. 3, (2020) 034503, [arXiv:1910.04827 \[hep-lat\]](#).
- [76] P. Bicudo, N. Cardoso, L. Mueller, and M. Wagner, “Computation of the quarkonium and meson-meson composition of the $\Upsilon(nS)$ states and of the new $\Upsilon(10753)$ Belle resonance from lattice QCD static potentials,” *Phys. Rev. D* **103** no. 7, (2021) 074507, [arXiv:2008.05605 \[hep-lat\]](#).
- [77] P. Bicudo, N. Cardoso, L. Mueller, and M. Wagner, “Study of $I = 0$ bottomonium bound states and resonances in S, P, D, and F waves with lattice QCD static-static-light-light potentials,” *Phys. Rev. D* **107** no. 9, (2023) 094515, [arXiv:2205.11475 \[hep-lat\]](#).
- [78] S. Godfrey and N. Isgur, “Mesons in a Relativized Quark Model with Chromodynamics,” *Phys. Rev. D* **32** (1985) 189–231.
- [79] W. Kilian and T. Mannel, “QCD corrected $1/m$ contributions to BB -mixing,” *Physics Letters B* **301** no. 4, (1993) 382–392.

- [80] M. Neubert, “Heavy-quark symmetry,” *Physics Reports* **245** no. 5-6, (1994) 259–395.
- [81] M. Neubert, “Heavy-Quark Effective Theory,” [arXiv:hep-ph/9610266](#).
- [82] V. Burkert *et al.*, “Note on the definitions of branching ratios of overlapping resonances,” *Phys. Lett. B* **844** (2023) 138070, [arXiv:2207.08472](#) [hep-ph].
- [83] M. T. Hansen and S. R. Sharpe, “Multiple-channel generalization of Lellouch-Lüscher formula,” *Phys. Rev. D* **86** (2012) 016007, [arXiv:1204.0826](#) [hep-lat].